Macromolecules

Article

pubs.acs.org/Macromolecules

Electric Birefringence of Aqueous Solutions of a Rigid Polyelectrolyte. Polarization Mechanisms and Anomalous Birefringence Signals

Hernán A. Ritacco,*[,†] Marcos Fernández-Leyes,[†] Claudia Domínguez,[†] and Dominique Langevin[‡]

[†]Instituto de Física del Sur (IFISUR), Consejo Nacional de Investigaciones Científicas y Técnicas (CONICET) and Departamento de Física, Universidad Nacional del Sur (UNS), Av LN Alem 1253, 8000 Bahía Blanca, Argentina

[‡]Laboratoire de Physique des Solides, CNRS, Université Paris Saclay, Université Paris-Sud, Bât 510, 91405 Orsay, France

Supporting Information

ABSTRACT: We present an electric birefringence study of aqueous solutions of an intrinsically rigid polyelectrolyte, xanthan, and of mixed solutions with an oppositely charged surfactant, DTAB. The stationary electric birefringence as well as built-up and decay processes give information on the polarization mechanisms of the polyelectrolyte and on the role played by counterions. By adding a cationic surfactant (DTAB), that replaces the small Na^+ counterions of the polymer, we could obtain further insights into the role of condensed counterions in these mechanisms. In some cases, anomalous birefringence signals appear, revealing a new polarization mechanism likely due to field-induced interactions within polymer−surfactant aggregates.

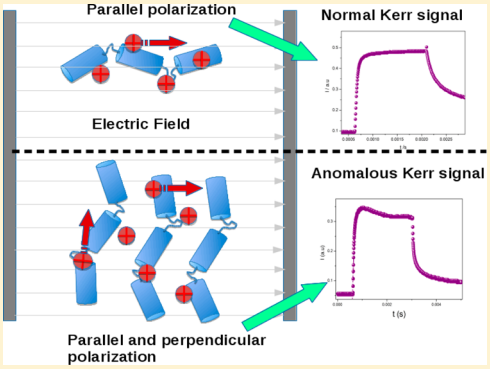

1. INTRODUCTION

Polyelectrolytes are macromolecules that behave as electrolytes: when dissolved in water, they dissociate into multivalent macroions and small counterions. Polyelectrolyte solutions are characterized by strong electrical interactions between the macroions and their counterions.[1] These interactions play important roles in the behavior of biopolymers such as nucleic acids or proteins, and of mixed solutions with oppositely charged entities, found in many areas of applied research. For instance, when polyelectrolytes are mixed with oppositely charged surfactants, polyelectrolyte−surfactant aggregates are formed, with applications in paints and coatings, food, pharmaceuticals, cosmetics, detergency, and oil recovery.[2] The electrical interactions in these systems are also important in the structure and the assembly kinetics of polyelectrolytes multilayers built onto flat surfaces, micro- and nanoparticles, liposomes, and other charged surfaces by means of the layer-by-layer technique.[3]

Current models for polyelectrolyte solutions are generally based on counterion condensation, an idea first introduced by Imai and Onishi[4] as well as Oosawa[5] and developed later by Manning. After Manning's important contributions, the theory is commonly known as Manning condensation theory.[6−8] The basic idea underlying this model is that when the charge density on a linear polyelectrolyte chain exceeds a critical value, such that the electrical potential along the chain reaches the value k_BT/e, k_B being the Boltzmann constant, T the absolute temperature, and e the electron charge; the exceeding charge is neutralized by the counterions. Part of the counterions then condenses onto the polymer chain, close to the charged group, so that the chain potential does not exceeds k_BT/e.

Electric birefringence (Kerr effect) is a very useful and sensitive technique for studying the interactions between the macroions and their counterions.[9] In the technique, an electric field is applied to a liquid and the time evolution of the generated birefringence is measured. In the presence of an electric field, the atmosphere of small ions around the polyelectrolyte chain is displaced from its equilibrium position producing a dipole which drives the orientation of the chain in the field. It is accepted that the counterion polarization is the dominant contribution (over that of other induced and permanent dipoles) on the orientation mechanism of polyelectrolytes.[10−16] It has also been shown theoretically that condensed counterions lead to important contributions to the polarization of the macroion.[17−24] Electric birefringence experiments in sodium polystyrenesulfonate (NaPSS) aqueous solutions evidenced two contributions of opposite signs due to the counterions polarization.[13−15] In order to interpret the observations, it was assumed that condensed counterions polarize along the main chain and that free counterions (or loosely bound) polarize perpendicularly, being the contribution to the birefringence signal of each polarization mechanism of opposite sign. The same conclusion was reached for a flexible polyelectrolyte, a sodium salt of polyacrylamide-acrylamido

Received: June 10, 2016
Revised: July 20, 2016
Published: July 29, 2016

DOI: 10.1021/acs.macromol.6b01240
Macromolecules 2016, 49, 5618−5629

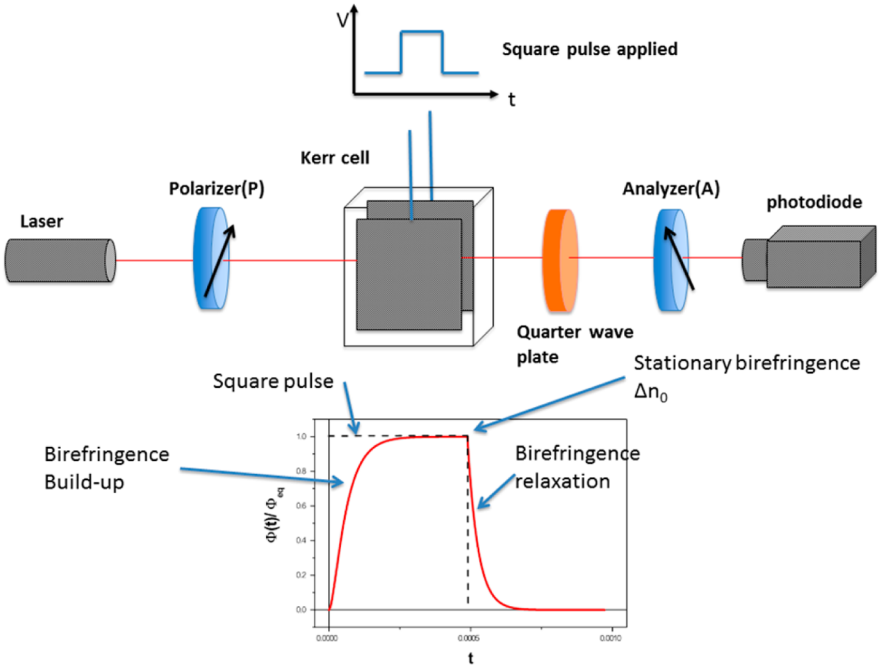

Figure 1. Kerr setup scheme and typical signal.

methylpropanesulfonate (PAMPS),[25] at concentrations above the chain overlap concentration. In this work, the birefringence signal could be changed from negative to positive by adding an oppositely charged surfactant that replaces the polymer counterions and binds to the chain. No change of sign was observed when a simple salt (NaBr) was added instead of the surfactant, in which case no ion condensation occurs. In general, however, the main contribution to the electric polarizability comes from the polarization of condensed counterions along the polymer chain.[12]

Negative electrical birefringence has also been observed in dispersions of rods such as fd viruses[26] that align perpendicularly to the applied electric field, under certain conditions and at concentrations above the overlap concentration. It has been proposed that the anomalous signals are due to field-induced interactions among the rods,[27] the perpendicular polarization dominating over the parallel polarization when the diameter of the rod assembly exceeds the rod length. Anomalous birefringence was also reported in dilute mixtures of charged rod-like and spherical colloids.[28] It was suggested in this case that the accumulation of spherical particles on one side of the rod gives rise to asymmetric electro-osmotic flows which induce a negative torque. Anomalous birefringence signals were also reported in other charged systems including concentrated micellar solutions, clay, and fibril dispersions in aqueous solvents. More information can be found in a recent review.[29]

In this paper we present and examine birefringence data for an intrinsically rigid polyelectrolyte, xanthan, pure and mixed with small amounts of an oppositely charged surfactant, dodecyltrimethylammonium bromide (DTAB). DTAB condenses on xanthan chains in a cooperative manner above a well-defined surfactant concentration called CAC,[2] allowing us to control the fraction of condensed counterions. The results are examined in the light of a simple phenomenological model based on Manning's condensation model, considering that the polarization of condensed counterions is the main mechanism for the orientation of the polyelectrolyte in the electric field. From this simple model, we are able to determine the values of anisotropies of optical and electric polarizabilities and propose an explanation for the anomalous birefringence observed in some mixed xanthan−DTAB solutions. Additionally, the measured birefringence rise and decay relaxation give further information on the polarization mechanisms of polyelectrolytes.

2. METHODS AND MATERIALS

2.1. Transient Electric Birefringence (TEB). When an electric field E is applied to an isotropic liquid, the liquid becomes birefringent; i.e., the refractive index becomes anisotropic. This phenomenon is called Kerr effect, and it is due to the orientation of the molecules in the electric field. Because of the orientation of the molecules, the refractive indices measured parallel, $n_{\|}$, and perpendicular, $n_{\perp}$, to the field are different. The birefringence is defined as $\Delta n = n_{\|} - n_{\perp}$ and can be positive or negative. As long as the electric field is applied, the birefringence increases until it reaches a stationary value, Δn_0, which corresponds to the equilibrium orientation distribution of the molecules at the given electric field value. For low electric field intensities and the majority of liquids, the induced birefringence is a linear function of E^2, $\Delta n_0 = BE^2\lambda$, being λ the light wavelength and B is a constant which is called the Kerr constant.

The experimental setup for measuring the electrically induced birefringence is similar to the one described previously.[30] The setup is shown schematically in Figure 1 with a typical birefringence signal obtained with a pulse of electric field, showing the buildup and the decay relaxation of the birefringence.

The cell containing the liquid sample has two quartz windows and two parallel metal plates (stainless steel, 40 × 50 mm) at a distance of 2 mm, acting as electrodes. These electrodes are connected to a pulse generator (homemade) capable of producing electric square pulses from 100 to 2000 V. The pulse width can be varied between microseconds and several milliseconds, with rise and decay times less than 200 ns. The light source is a He−Ne laser (15 mW), coupled to a polarizer with its slow axes oriented at 45° with respect to the applied electric field. A second polarizer, the analyzer, is located just before a photodiode (Thorlabs DET10C) and oriented to be in a crossed position with respect to the first polarizer. In this way no light hits the detector when the electric pulse is off. When the electric pulse is switched on, birefringence is generated in the sample, and some light reaches the photodiode. The Kerr signal is recorded via a digital

DOI: 10.1021/acs.macromol.6b01240
Macromolecules 2016, 49, 5618−5629

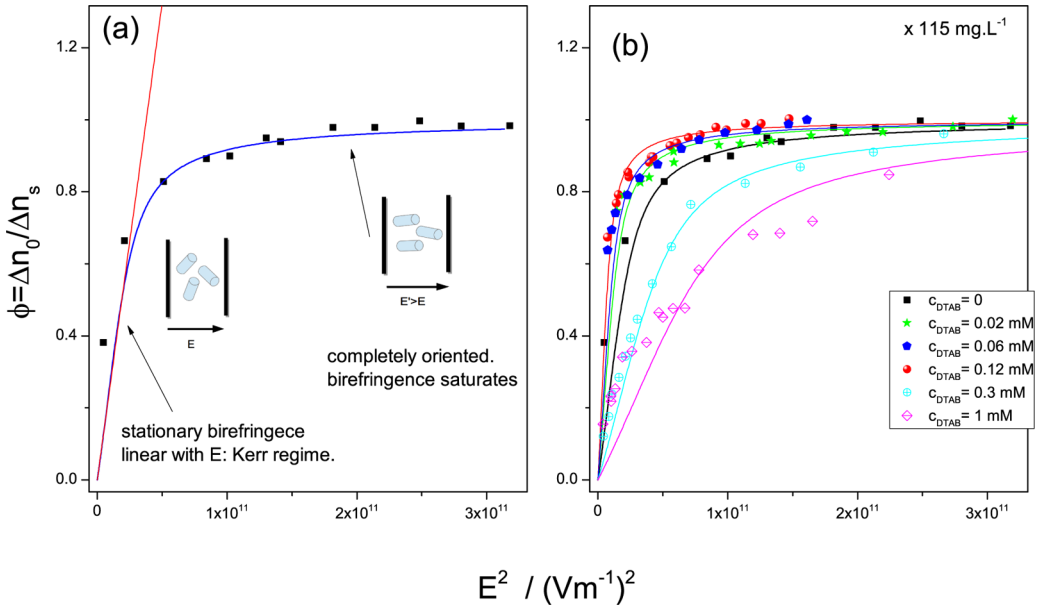

Figure 2. (a) Electric birefringence versus the square of the field E for a 115 mg/L xanthan aqueous solution. The blue line is a fit with eq 7, and the red line corresponds to eq 8. (b) The same curves as in (a) as a function of DTAB concentration.

oscilloscope and a computer. In order to measure the sign of the birefringence, a quarter-wave plate is placed between the sample and the second polarizer, and the analyzer is rotated a small angle with respect to the crossed position.

2.2. Materials. Xanthan is an extracellular polysaccharide produced by fermentation of the microorganism *Xanthomonas campestris*. Its structure is shown in the Supporting Information. The polymer has been obtained from International Drilling Fluids (IDF) and was purified by microfiltration at low flow rate. The weight-average molecular weight, M_w, of the sample was measured by multiangle light scattering: $M_w = 1.8 \times 10^6$ g mol^{-1}. The monomer mass is 930 g, the number of charges per monomer $f = 1.5$, and the monomer size $b = 1$ nm.[31] The conformation of xanthan molecules has been studied with a number of techniques including light and neutron scattering, circular dichroism, viscosity, and others[32−42] and also electric birefringence.[43] Xanthan molecules are usually found in a quite rigid double-helix configuration, the intrinsic persistence length being $l_p^0 = 140$ nm.[44] A less rigid single-helix configuration can also be obtained, with a persistence length of 40 nm.[40,44]

The surfactant used is dodecyltrimethylammonium bromide (DTAB), which is a cationic surfactant, purchased from Sigma-Aldrich and purified twice by recrystallization in mixtures of 10 mL of ethyl acetate and 1 mL of ethyl alcohol. The solutions were prepared in Millipore Milli-Q water. Because of limited amounts of the xanthan samples, we have used only two polyelectrolytes concentrations, $c_p = 60$ mg L^{-1} and $c_p = 115$ mg L^{-1}, both above the overlap concentration (see section 4.1). All birefringence measurements were carried out at 298 K.

3. RESULTS

3.1. Stationary Birefringence. Figure 2 shows the stationary birefringence as a function of the electric field strength for an aqueous solution of xanthan with $c_p = 115$ mg L^{-1}. The birefringence saturates at large electric field intensities. This behavior is generally interpreted as the molecules been completely oriented in the electric field: no further orientation is possible even if the electric field intensity is increased, and then the birefringence remains constant (see inset drawing in Figure 2a).

For surfactant free solutions, and at the concentration of 115 mg L^{-1}, the birefringence at saturation is $\Delta n_s = (4.1 \pm 0.2) \times 10^{-7}$. The variation of the stationary birefringence of 60 mg L^{-1} solutions with electric field is similar (see Supporting Information), being the birefringence at saturation slightly smaller: $\Delta n_s = (3.4 \pm 0.3) \times 10^{-7}$. The birefringence at saturation depends on surfactant concentration (see Supporting Information). The values are given in Table 1.

Table 1. Birefringence at Saturation for the Two Polymer Concentrations and Various Surfactant Concentrations

c_{DTAB} (mM)	$\Delta n_s \times 10^7$ for $c_p = 60$ mg/L	$\Delta n_s \times 10^7$ for $c_p = 115$ mg/L
0.01	2.9 ± 0.2	
0.02		2.1 ± 0.2
0.03	3.3 ± 0.2	
0.05	3.4 ± 0.2	
0.06		2.3 ± 0.2
0.08	3.4 ± 0.3	
0.1	3.3 ± 0.4	
0.12		2.0 ± 0.2
0.2	2.8 ± 0.3	
0.3		5.2 ± 0.2
0.4	3.2 ± 0.2	
1		5.6 ± 0.5

3.2. Birefringence Relaxation. The decay relaxations were measured for electric field strengths between 200 and 800 V/mm.

3.2.1. Surfactant Free-Xanthan Solutions. For dilute solutions of monodisperse, rod-like rigid molecules, one has[45]

$$\frac{\Delta n(t)}{\Delta n_0} = A_r e^{-t/\tau_r} \quad (1)$$

The time evolution of the birefringence is in this simple case, described by a single exponential with relaxation time $\tau_r = 1/(6D_r)$, D_r being the rotation diffusion coefficient. Δn_0 is the value of the birefringence when the stationary regime is reached.

Figure 3 shows a typical relaxation curve for a surfactant-free xanthan solution. The recorded relaxation signals could not be fitted with a single exponential. We then used two approaches to

DOI: 10.1021/acs.macromol.6b01240
Macromolecules 2016, 49, 5618−5629

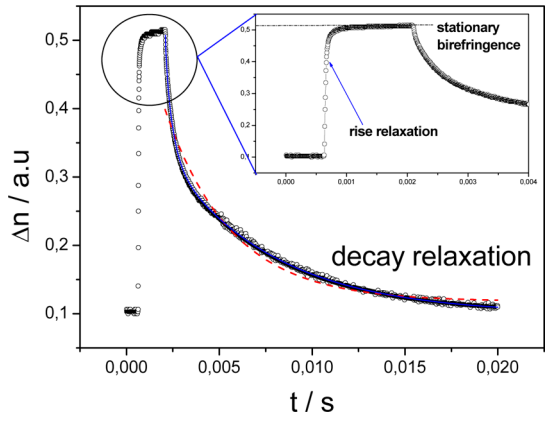

Figure 3. Typical birefringence signal where the rise and decay of the signal can be seen. Xanthan 115 mg L^{-1}, E = 400 V/mm. The inset shows the value of the stationary birefringence for the applied field. The dashed line (red) correspond to fitting with a simple exponential function; the solid line (blue) is the fitting with a multiexponential (three) function.

analyze the relaxation curves: multiexponential and stretched exponentials, as explained below.

The relaxation curves were first fitted with a sum of exponentials of decay times τ_i and amplitudes A_i. The minimum number of characteristic relaxation times needed to obtain good fits was three. We then used

$$\frac{\Delta n(t)}{\Delta n_0} = A_1 e^{-t/\tau_1} + A_2 e^{-t/\tau_2} + A_3 e^{-t/\tau_3} \quad (2)$$

The values of the three relaxation times are shown in Figure 4 versus the applied electric field and for the two polymer concentrations, c_p = 60 and 115 mg L^{-1}. The values of the corresponding amplitudes are shown in the Supporting Information.

The relaxation times for c_p = 60 mg L^{-1} are slightly field dependent, the longest time τ_3 being about 10 times larger than τ_2 and 100 times larger than τ_1. The amplitudes do not significantly change with the field, those for the longest time being about twice those for the shorter ones (see Supporting Information). The relaxation times for the more concentrated xanthan solution, c_p = 115 mg L^{-1}, depend less on field strength. The longest time τ_3 is 6 times smaller than for c_p = 60 mg L^{-1} while the other times are similar. The amplitudes vary more than with the more dilute solutions, by factors of about 2 (see Supporting Information).

The method of stretched exponentials was also proposed for analyzing birefringence relaxation for solutions of flexible polyelectrolytes.[46] The curves were then fitted with

$$\Delta n(t) \sim \exp\left(-\frac{t}{\tau}\right)^{\beta} \quad (3)$$

For the more diluted xanthan solution c_p = 60 mg L^{-1}, the method leads to a relaxation time that depends on field strength with an extrapolated to E = 0 value of 3 ms, close to τ_2. The exponent β was found to be field independent with a mean value of β = 0.29 ± 0.05. For the higher polymer concentration, c_p = 115 mg L^{-1}, the relaxation time depends also on the electric field strength with a value extrapolated to zero field of τ = 0.5 ms. For this polymer concentration, the exponent β also depends on the electric field intensity varying between 0.24 at small E and 0.4 for the highest field strength (E = 700 V/mm) (see Supporting Information).

3.2.2. Mixed Xanthan–DTAB Systems. As for pure xanthan solutions, we analyzed the relaxation curves by fitting them with three exponentials and stretched exponentials (eqs 2 and 3). The fits were made for c_p = 60 and 115 mg L^{-1}, several electric field strengths and several DTAB concentrations, below the isoelectric point, c_{ip} (concentration at which the number of charges from DTAB equals those of the polyelectrolyte), close to this point and above the c_{ip}. The complete results are shown in the Supporting Information.

For both polyelectrolytes concentrations, the values of the three characteristics times are rather independent of the electric field (see Supporting Information). Below the CAC (~0.1 mM), the relaxation times are close to those measured for pure xanthan solutions and decrease appreciably above the CAC, especially for the solutions with c_p = 115 mg L^{-1}. The values of the three times are shown in Figure 5 as a function of DTAB concentration.

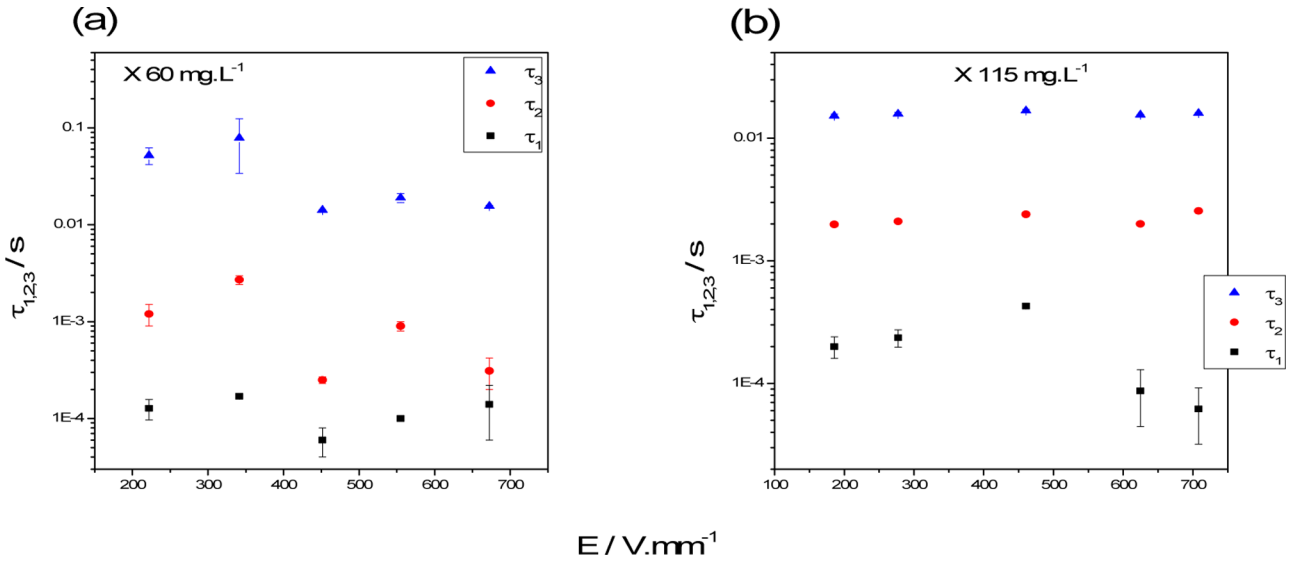

Figure 4. Relaxation times for xanthan 60 and 115 mg L^{-1} as a function of field strength, E, obtained by multiexponential fitting.

DOI: 10.1021/acs.macromol.6b01240
Macromolecules 2016, 49, 5618−5629

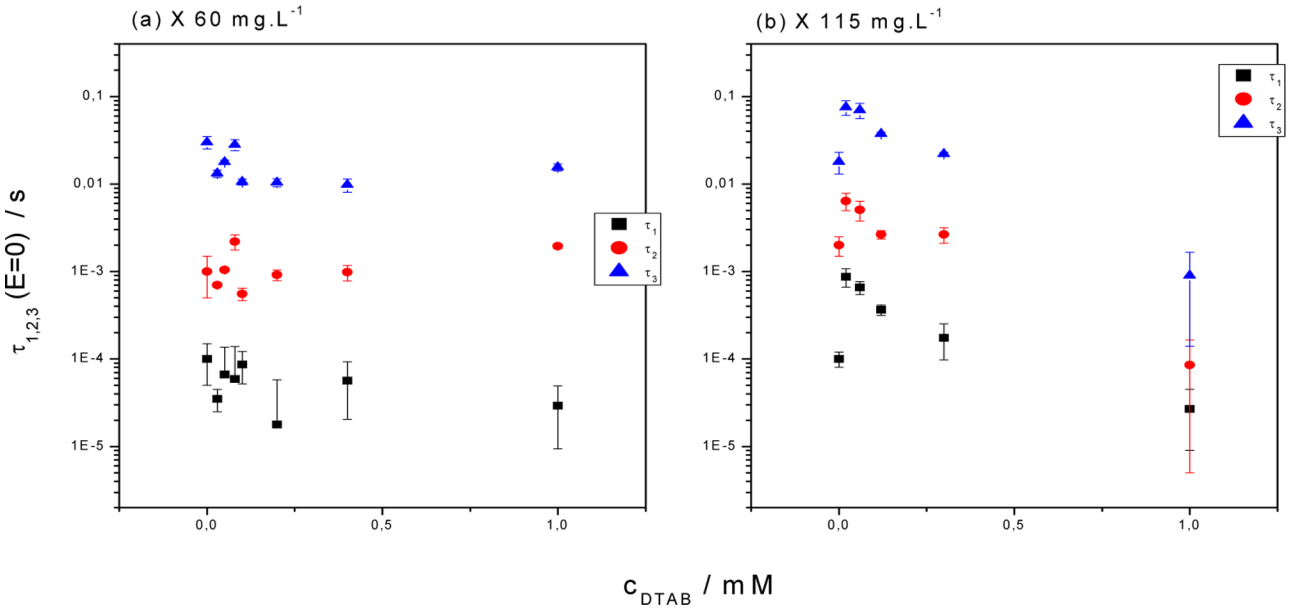

Figure 5. Relaxation times extrapolated to $E = 0$ for xanthan (a) 60 and (b) 115 mg L^{-1} as a function of surfactant concentration obtained by multiexponential fitting.

The relaxations were also analyzed using stretched exponentials (see Supporting Information). The relaxation time is close to τ_2 as for surfactant-free solutions, and β is small: $0.27 < \beta < 0.48$.

3.3. Birefringence Buildup and Anomalous Birefringence Signals. *3.3.1. Anomalous Signals.* In Figure 6 we show a birefringence signal for the mixed system xanthan 115 mg L^{-1} and 0.02 mM DTAB obtained at very high field strength, 750 V/mm.

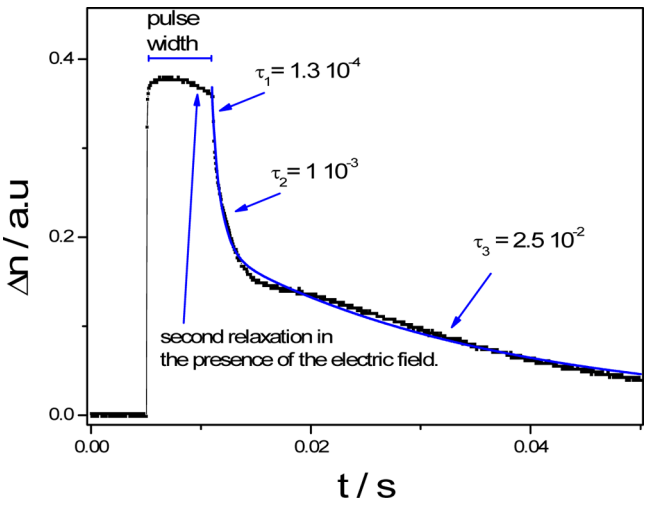

Figure 6. Birefringence signal for xanthan 115 mg L^{-1} and 0.02 mM DTAB for $E = 750$ V/mm. An "anomalous" relaxation processes can be seen when the electric field is still on. The line (blue) corresponds to a multiexponential fitting (three relaxation times).

The decay relaxation was fitted with three relaxation times as in Figure 3. During the birefringence buildup process, the birefringence first increases with time and then decreases, evidencing a negative contribution with a longer characteristic time. Buildup curves such as that of Figure 6 were observed in other systems and are generally called *anomalous*.[29]

The anomalous signals are not present for xanthan−DTAB solutions with $c_p = 60$ mg L^{-1} whatever the applied field. For the more concentrated xanthan solution, $c_p = 115$ mg L^{-1}, and for DTAB concentrations less than c_{ip}, anomalies are present only at high field strengths, while for $c_{DTAB} > c_{ip}$ the anomalous signals are present at all field intensities (from 100 to 800 V mm^{-1}) (see Supporting Information).

In Figure 7 we present four signals for $c_p = 115$ mg L^{-1} and $c_{DTAB} = 1$ mM for different electric field strengths. In these signals, one can see that the negative contribution to the birefringence increases as E increases. The anomalous behavior become more visible and appears faster at high field and high polymer and DTAB concentrations (see Supporting Information for more complete results).

4. DISCUSSION

4.1. Polymer Conformation. *4.1.1. Polymer Aqueous Solutions.* Polymers, even rigid ones, do not have rod-like chain conformations. Let us first discuss the case of dilute solutions. The electrical birefringence is then sensitive to the end-to-end distance R of polymer chains. If we denote by L the extended chain length and l_p its persistence length, the end-to-end distance is

$$R = l_p(L/l_p)^n \tag{4}$$

with $\nu = 2/3$ in good solvent conditions.[1] The persistence length l_p of xanthan obtained by single molecule observation with atomic force microscopy[47] and other techniques[37,40] is of the order of 500 nm, larger than the intrinsic persistence length l_p^0 quoted earlier (140 nm). This is because the persistence length contains an ionic contribution l_p^e:

$$l_p = l_p^0 + l_p^e \tag{5}$$

For intrinsically rigid chains, the electrostatic contribution to the persistence length is given by the Odijk−Skolnick−Fixman (OSF) theory,[48−50] $l_p^e = l_b/4\kappa^2A^2$, where κ is the inverse Debye length: $\kappa = (4\pi l_b fc)^{1/2}$, l_b is the Bjerrum length, A is the distance between adjacent charges, and f is the number of charges per

DOI: 10.1021/acs.macromol.6b01240
Macromolecules 2016, 49, 5618−5629

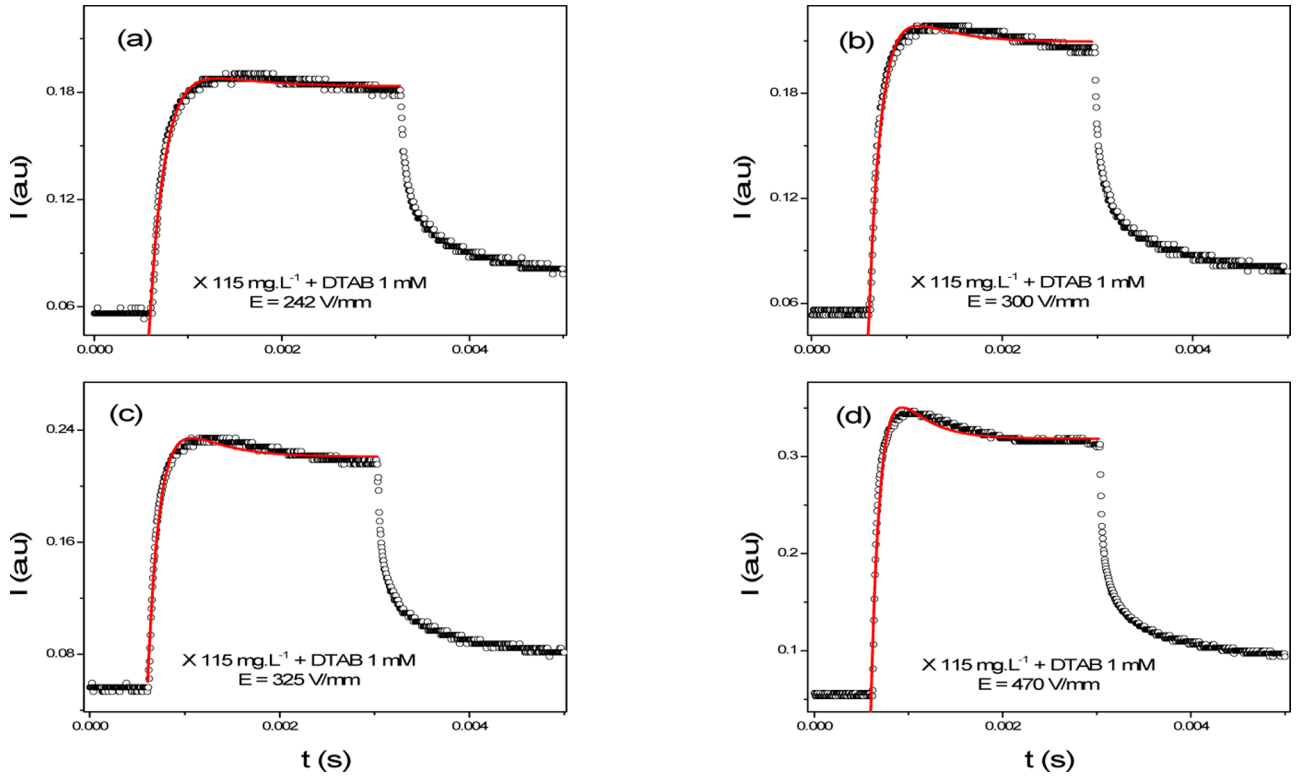

Figure 7. Anomalous birefringence signals for 115 mg L^{-1} xanthan + 1 mM DTAB solutions and different field strengths. (a) E = 242 V/mm; (b) E = 300 V/mm; (c) E = 325 V/mm; (d) E = 470 V/mm. The lines are the fits with eq 15.

monomer. For a xanthan concentration c_p = 60 mg L^{-1}, the calculated electrostatic contribution is $l_p^e \sim 680$ nm, and for c_p = 115 mg L^{-1}, $l_p^e \sim 340$ nm. One obtains therefore $l_p \sim 700$ and 500 nm for the two concentrations studied, respectively.

The number of monomers of the xanthan studied is $N_m = 1.8 \times 10^6/930 \sim 2000$, and with a monomer length b = 1 nm, $L \sim 2$ μm. Using eq 4, we find an end-to-end distance R of about 1.2 μm at the concentrations used: the polymer is almost completely extended. The distance between charges A is $b/f \sim$ 0.67 nm, smaller than but close to the Bjerrum length l_B = 0.7 nm. The Manning parameter $\xi_M = l_B/A$ is therefore close to one, and only a few counterions $(1 - 1/\xi_M \sim 4\%)$ are condensed along the polymer chain.[6−8]

The persistence length calculated using eq 5 is larger than L for c_p < 10 mg L^{-1}. We can therefore use the length L to estimate the overlap concentration: $c^* = M_w/(\mathcal{N}L^3)$, $\mathcal{N}$ being the Avogadro number. This leads to $c^* \sim 0.4$ mg L^{-1}, well below the concentrations used. The solutions are also well below the concentrated regime, the viscosity of the more concentrated solution being only twice that of water. The distance ξ between overlap points can also be estimated: ξ varies as $c^{1/2}$[1] and is equal to R at c^*. Because R changes with concentration due to progressive electrostatic self-screening and chain folding, we used the c^* for an end-to-end distance R at the concentrations used: $c^* \sim 3$ mg L^{-1}. We thus find ξ = 220 nm for 60 mg L^{-1} and 160 nm for 115 mg L^{-1}. Such values are in good agreement with those experimentally determined for xanthan.[51]

4.1.2. Mixed Solutions with DTAB. When DTAB is added to xanthan solutions, there is a strong electrostatic attraction between the charged groups as well as attractive hydrophobic interactions between surfactant and polymer chains, leading to cooperative bulk complexation. The surfactant DTA^+ ions replace the small Na^+ around the polyelectrolyte chain and bind (condense) to the chain above a surfactant concentration called the critical aggregation concentration (CAC), which can be several orders of magnitude below the critical micelle concentration (CMC) of the surfactant. Note that surfactant binds to the polymer below the CAC, but this binding is noncooperative and concerns a very small fraction of ions.[2] The binding degree β_d (ratio of the number of polymer charges bound to surfactant to the total number of polymer charges) increases and saturates ($\beta_d \sim 1$) at a surfactant concentration T2 which depends on the cooperativity of the complexation: the more cooperative the complexation, the closer this concentration to the CAC.[52] The CAC at which the cooperative binding of DTAB ions to xanthan starts is not expected to depend much on polymer concentration in the small range probed.[52] Surface tension determinations showed that for xanthan and DTAB the CAC is about 0.1 mM.[53] This is comparable to the value measured with a similar surfactant using binding isotherms.[54]

Because of surfactant binding, the polymer becomes less charged above the CAC and coils progressively. For the largest surfactant concentration used (1 mM), the electrostatic persistence length drops to 62 nm, so the total persistence length is only 200 nm and $R \sim 800$ nm instead of 1.2 μm.

Furthermore, the chain becomes hydrophobic due to the presence of the surfactant chain along its backbone. When the amount of surfactant and polymer ions are equal (c_{ip}), a full neutralization of the chain can occur, followed by precipitation. For xanthan 60 mg L^{-1} $c_{ip} \sim 0.1$ mM, and for xanthan 115 mg L^{-1} $c_{ip} \sim 0.18$ mM. Note however that the precipitation concentration is not always equal to the c_{ip}[52] and that precipitation is not seen if the polymer concentration is too small.[2] Here, partial precipitation under the form of filamentous gels sticking to the surface of the solution container were

DOI: 10.1021/acs.macromol.6b01240
Macromolecules 2016, 49, 5618−5629

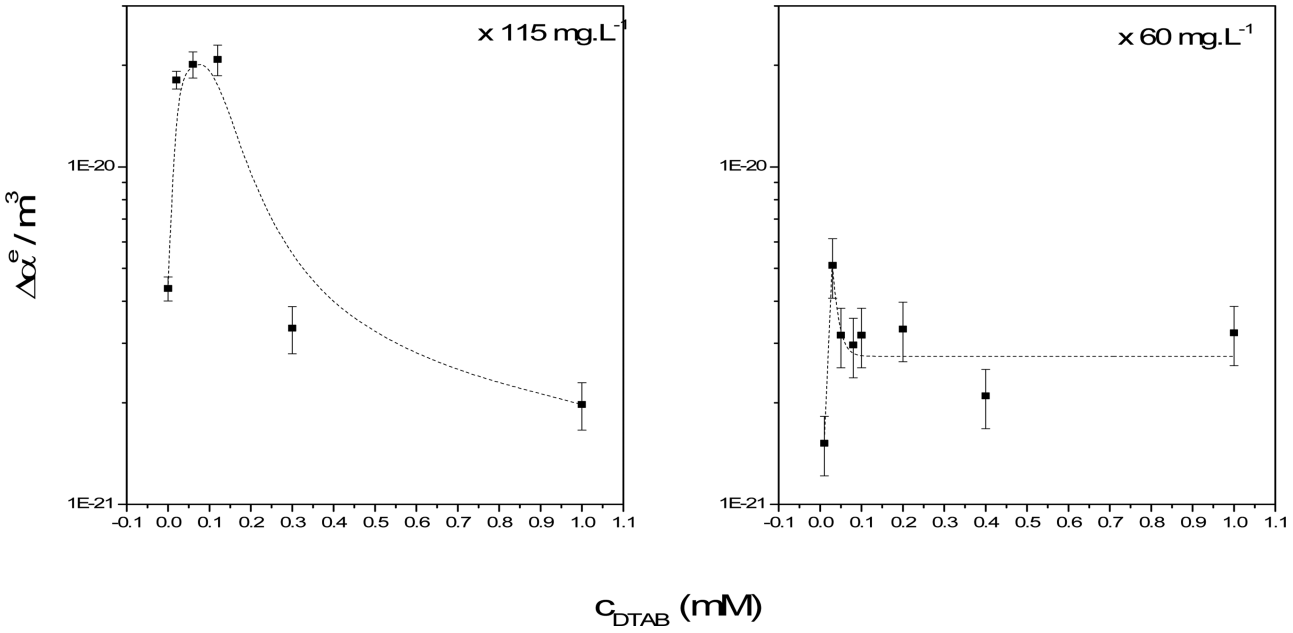

Figure 8. Electric polarizability from the analysis of stationary birefringence as a function of DTAB concentration for xanthan 115 mg L^{-1} solutions.

observed for 115 mg L^{-1} around 0.2−0.3 mM DTAB but disappeared above. Precipitates were never observed with the more dilute polymer solution.

4.2. Stationary Birefringence. *4.2.1. Pure Xanthan Solutions.* Figure 2 shows the stationary birefringence as a function of the electric field strength for an aqueous solution of xanthan with c_p = 115 mg L^{-1}. The birefringence saturates at intermediate electric field intensities. When the molecules are completely oriented in the electric field, the birefringence remains constant (see Figure 2a). The optical polarizability of the molecules can then be deduced as follows. For completely oriented molecules in the electric field, the birefringence is given by

$$\Delta n_s = \frac{2\pi}{9n}(n^2+2)^2 N\Delta\alpha^0 \tag{6}$$

n being the solution refraction index, Δn_s the birefringence when all the molecules are fully oriented parallel to the field, N the number of molecules per unit volume, and $\Delta\alpha_0$ the intrinsic optical polarizability anisotropy of the macromolecule, difference between optical polarizabilities parallel and perpendicular to the applied electric field: $\Delta\alpha^0 = \alpha^0_{\parallel} - \alpha^0_{\perp}$.

For xanthan solutions, $\Delta n_s = 3.4 \times 10^{-7}$ and 4.1×10^{-7} for 60 and 115 mg L^{-1}, respectively (see section 3.1). Using eq 6 with $n \sim 1$, we obtain respectively $\Delta\alpha^0 = 2.7 \times 10^{-27}$ and 1.7×10^{-27} m^3. Note that this analysis is valid for dilute rod-like polymer solutions. The calculated values of $\Delta\alpha^0$ should therefore be considered as indicative. The values of the polarizabilities are probably influenced by the coiling of the macromolecules and, because the polymer solutions are semidilute, by the intermolecular interactions. This is probably why the optical polarizability $\Delta\alpha^0$ is smaller at the largest polymer concentration where the coiling is more important.

Let us discuss the issue of electrical polarizabilities. We will assume that as for other polyelectrolytes the chain orientation mechanism is dominated by the counterions around the main polymer axis.[12] The counterions can create dipoles either perpendicular or parallel to the main polymer axis. The birefringence is proportional to a time-dependent *orientation factor* $\Phi(t)$ which is the average value of the orientation factor $(3\cos^2\theta - 1)$, θ being the time-dependent angle between the molecule and the external electric field. When the stationary regime is reached, the orientation factor becomes time independent and equal to[17,18,55]

$$\Phi = \frac{\Delta n}{\Delta n_s} = \frac{3\int_{-1}^{1} v^2 \exp(\gamma v^2)\,dv}{2\int_{-1}^{1}\exp(\gamma v^2)\,dv} - \frac{1}{2} \tag{7}$$

where $v = \cos\theta$ and $\gamma = \Delta\alpha^e E^2/k_B T$, $\Delta\alpha^e$ being the difference in the counterion polarizabilities along and perpendicular to the main polymer axis, k_B the Boltzmann constant, and T the absolute temperature. For very low external electric fields, the orientation factor reads

$$\Phi = \frac{\Delta\alpha^e E^2}{15 k_B T} \tag{8}$$

The fit with eq 7 is shown in Figure 2a. From these fittings we obtain $\Delta\alpha^e$, which is equal to 4×10^{-21} m^3 for c_p = 115 mg L^{-1}. Similar fits (see Supporting Information) lead to $\Delta\alpha^e = 1 \times 10^{-21}$ m^3 for c_p = 60 mg L^{-1}. These polarizability anisotropies are much smaller than for polystyrenesulfonate (5×10^{-18} m^3 in ref 12), but the structure of the polymer molecule is different, the charges of xanthan being located in side chains (see Supporting Information).

Let us further assume as in ref 12 that the main contribution to the electric polarizability comes from the polarization of condensed counterions along the polymer chain and that the displacement of free counterions has no effect on the macromolecule polarizability. Following ref 12, we can write

$$\Delta\alpha^e = \alpha^e_{\parallel} - \alpha^e_{\perp} = \alpha^e_{\parallel} = \frac{e^2 f(1 - 1/\xi_M) N_m R^2}{k_B T} \tag{9}$$

where e is the electron charge and N_m the number of monomers of the polymer chain and assuming that $\alpha^e_{\perp} = 0$. With the values of the parameters of section 4.1, we find $\Delta\alpha^e \sim 4 \times 10^{-18}$ m^3. This value is much larger than those obtained above from the fits

DOI: 10.1021/acs.macromol.6b01240
Macromolecules 2016, 49, 5618−5629

with eq 7. However, many approximations were made during the derivation of eq 9, and although the dependence on the number of condensed counterions and chain size might be correct, the validity of the prefactors can be doubted as pointed out in ref 12.

4.2.2. Mixed Solutions with DTAB. Fits with eq 7 were also performed for the measured stationary birefringence at several DTAB concentrations below and above the isoelectric point. The values obtained $\Delta\alpha^e$ are shown in Figure 8 as a function of surfactant concentration: $\Delta\alpha^e$ exhibits a maximum close to the isoelectric point.

$DTAB^+$ ions mix with Na^+ ions in the vicinity of the polymer chain and progressively bind to chain. Since we assumed that the electrical polarizability is due to the condensed counterions, the initial increase in electric polarizability is likely due to this binding (ξ_M decreases, see eq 9). The maximum value of $\Delta\alpha^e$ is about 5 times larger than without DTAB for both polymer concentrations. Since the isoelectric point c_{ip} is close to the CAC, all the surfactant ions should be condensed onto the polymer chain when $\Delta\alpha^e$ is maximum, and the increase of $\Delta\alpha^e$ should have been of a factor 25 instead (since only 4% of the counterions are condensed in the absence of surfactant). A possible origin of the discrepancy is the following: due to the very small polymer concentration, DTAB ions are in large excess and uncondensed ions increase the ionic strength, which decreases the end-to end distance R and as a consequence the electric polarizability (see eq 9).[22] However, the reduction factor is not sufficient to account for the observed increase of $\Delta\alpha^e$. Perhaps the discrepancy comes from missing factors in eq 9, which fails to account for the actual values of $\Delta\alpha^e$ in the absence of surfactant.

When the DTAB concentration increases above the c_{ip}, the ionic strength continues to increase and so does the degree of chain coiling. For 1 mM DTAB, we saw in section 4.1 that $R \sim$ 800 nm instead of 1.2 μm. Furthermore, the chain may start aggregating. Hence, the electric polarizability is expected to decrease, as observed. The decrease is much more important for 115 mg L^{-1} than for 60 mg L^{-1}, in agreement with the fact that aggregation appears quite limited in the more dilute polymer solutions.

Let us now discuss the stationary birefringence for the systems with anomalous signals. In this case, a new mechanism tends to orient the macromolecules perpendicular to the electric field, with a slower relaxation time depending on field strength (see signals a–d in Figure 7). Manning ascribes the negative contribution to the perpendicular polarizability of condensed counterions in an assembly of parallel rods of diameter of the order of the rod length.[27] This idea can be extended by saying that a counterion polarization perpendicular to main polymer axis arises when the condensed counterions are close enough to a neighbor macromolecule, so that the energy barrier for leaving the molecule onto which they are condensed can be overcome as these ions condense into an equivalent site on the neighbor molecule. When DTAB is added to sufficiently concentrated polymer solutions, aggregates indeed form when the surfactant concentration is increased.[53]

4.3. Birefringence Relaxation. When an electric field square pulse is applied to the liquid sample, the birefringence builds up in a certain time until it reaches a stationary value. This time known as *buildup* or *rise* time is related to the time needed to reach the orientation equilibrium for the molecules under the applied field. When the field is removed, the molecules relax to their original disordered isotropic state; the time needed in this case is known as the *relaxation* time. Both types of times give information on the dynamics of the orientation process and on the size and geometry of the molecules in the solution. In a TEB experiment, the induced birefringence, $\Delta n(t)$, is a function of time, t, and is given by the product of two factors[56]

$$\Delta n(t) \propto \Delta\alpha^0 \Phi(t) \tag{10}$$

$\Phi(t)$ being the time-dependent orientation factor.

Once the stationary value of the birefringence is reached and after the electric field is switched off, the generated birefringence relaxes. For dilute solutions of monodisperse, ellipsoidal rigid molecules the time evolution of the birefringence is described by a single exponential with relaxation time $\tau_r = 1/(6D_r)$, D_r being the rotation diffusion coefficient eq 1. The rotational diffusion time then allows estimating the molecular size.[45,57]

This result also applies to polymers in the case of very rigid chains $L < l_p$ and dilute solutions. The distribution of relaxation times is very narrow and the relaxation is well described by a single exponential. For flexible chains where $L \gg l_p$, again in the dilute regime, the relaxation follows a stretched exponential time variation[46] eq 3 with $\beta_{min} \sim 1/[\ 1 + 3(1 - \nu)]$;[46] for $\nu = 2/3$, $\beta_{min} = 0.5$.

The persistence length of xanthan is 500 nm for 60 mg L^{-1} and 400 nm for 115 mg L^{-1}. The extended chain length being 2 μm, the chain is coiled, with end-to-end distance of about 1.2 μm in both cases. The coiling is therefore limited, and the exponent β eq 3 should be close to 1.

4.3.1. Xanthan Solutions. The relaxation signals such as that shown in Figure 3 could not be fitted with a single exponential. This could be due to partial coiling. Furthermore, the polymer molecules are not monodisperse, the solutions are not dilute and intermolecular interactions cannot be neglected. Hence, it is not surprising that eq 1 cannot be applied. So far, multiexponential relaxation has been currently reported for electrical birefringence of polyelectrolyte solutions, but no clear insight into the origin of these relaxations has been proposed yet.[29,58,59]

In line with previous works, we fitted the relaxation curves with a sum of exponentials of decay times τ_i and amplitudes A_i (eq 2). The dependence of the relaxation times on the amplitude of the electric field is limited and might not be significant in view of the error bars. The relaxation times also depend little (within error bars) on the polymer concentration. This is likely because the characteristic lengths do not change appreciably between 60 and 115 mg/L.

It is not obvious to identify the nature of the relaxation processes involved. It should be remembered that birefringence comes from rotation of molecules following the electric field, hence one of these relaxation times should correspond to the rotational diffusion. For a rod-like molecule, the rotational relaxation time can be expressed by[60,61]

$$\tau = \frac{\pi\eta_0 l^3}{18k_B T}\left[\ln\left(2\frac{l}{d}\right) - 1.57 + 7\left(\frac{1}{\ln\left(2\frac{l}{d}\right)} - 0.28\right)^2\right]^{-1} \sim \frac{\pi\eta_0 l^3}{18k_B T}\left[\ln\left(\frac{l}{2d}\right)\right]^{-1} \tag{11}$$

where η_0 is the viscosity of the solvent and l and d are the length and diameter of the rod, respectively.

The three different times are of the order of 100 μs, 1 ms, and 30 ms. They would correspond to three different lengths

DOI: 10.1021/acs.macromol.6b01240
Macromolecules 2016, 49, 5618–5629

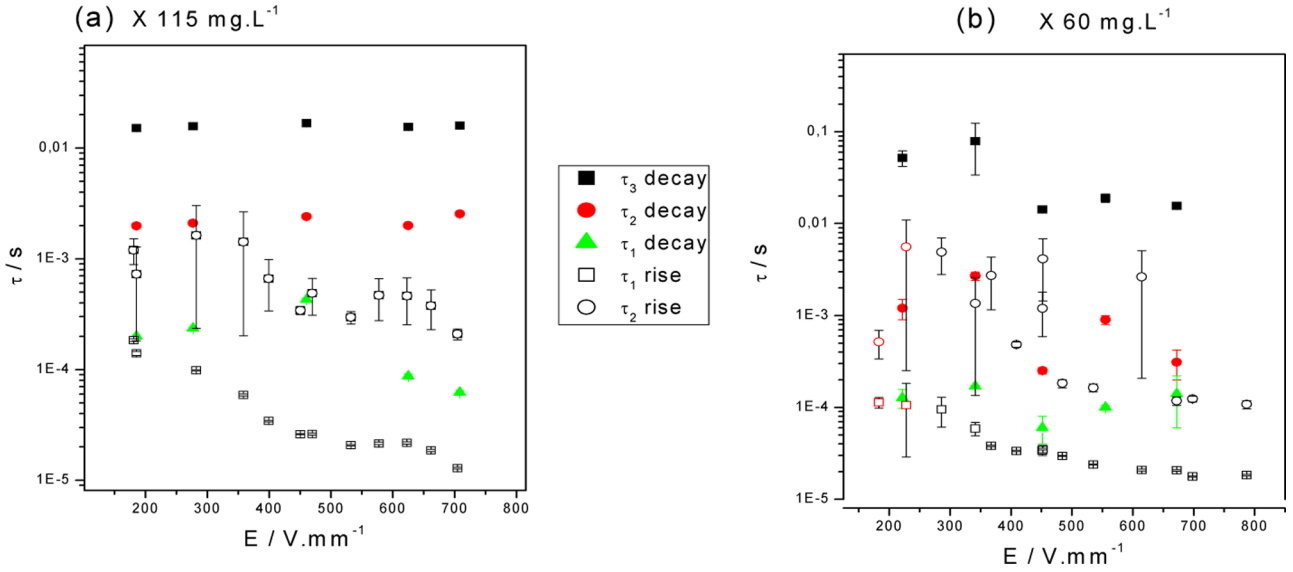

Figure 9. Characteristic times for birefringence rise and decay for xanthan 60 and 115 mg L^{-1} as a function of field strength, E, obtained by biexponential fitting.

according to eq 11; using the molecular diameter of d = 8 nm,[47] $l_1 \sim 220$ nm, $l_2 \sim 460$ nm, and $l_3 \sim 1.4$ μm. These lengths are respectively close to the correlation length ξ, the persistence length l_p, and the end-to-end distance R.

Degiorgio et al.[62,63] showed that the rotational relaxation times measured with electrical birefringence relaxation for a polymer chain with extended length L and persistence length l_p were consistent with the following expression:

$$\tau(x) = \tau_{rod}\left[x + \frac{e^{-2x} - 1}{2}\right]^{1.5} \frac{1 + 0.54\ln(1 + x)}{x^3} \qquad (12)$$

where τ_{rod} is the rotational time of a rod of length L and $x = L/2l_p$. With $l = L = 2$ μm, eq 11 gives $\tau_{rod} \sim 73$ ms. Using this value in eq 12 with the values of l_p for 60 and 115 mg L^{-1} (700 and 500 nm, respectively), one finds relaxation times τ of respectively 32 and 26 ms, close to the longest times measured and slightly larger for 60 mg L^{-1} as observed (Figure 4). We can therefore attribute the longer relaxation time to the rotation of the polymer molecule (as in the xanthan study of ref 43).

The shortest relaxation time τ_1 could correspond to the electric polarizability relaxation. Dielectric relaxation experiments with another rigid polymer, DNA, with similar molecular weight, have shown that at comparable concentrations, the largest dielectric relaxation time is very short, about 30 μs.[64] The diameter d of DNA molecules is smaller than that of xanthan molecules (2 nm instead of 8 nm), and the dielectric relaxation time is expected to decrease when d increases.[65] For xanthan, τ_{diel} is then expected to be even smaller than the shortest relaxation time τ_1, so τ_1 should have a different origin.

The relaxation times τ_1 and τ_2 could correspond to hairpin deformations as for microtubules[66] or to polymer segments orientation. One cannot also exclude the role of polydispersity, which is appreciable for this polymer.[47] As in previous works, it is then difficult to attribute well-defined mechanisms to the fastest relaxations.

Because the nature of the relaxations is likely different, it is not surprising to see that the stretched exponential fits lead to values of the exponent β much smaller than expected. In the following, we will discuss only the results of the multiexponential fitting.

4.3.2. Xanthan–DTAB Solutions. The relaxation times τ_3 diminish appreciably with surfactant concentration above the c_{ip} (Figure 5). Chain coiling could be responsible for part of the relaxation time decrease. Indeed, the relaxation time τ_3 is very sensitive to the size of the molecules. According to eqs 11 and 12, τ_3 should diminish by a factor of about 3, consistent with the determinations made for 60 mg L^{-1} solutions.

The decrease of τ_3 is more important for 115 mg L^{-1} solutions. According to partial precipitation observations, the aggregation near the isoelectric point is significant only for this more concentrated xanthan solution. This could explain why the longest relaxation times τ_3 diminish more appreciably with surfactant concentration above the c_{ip}. Indeed, if aggregates are present, this relaxation time will depend on the size of the aggregates rather than on the size of the individual molecules

One may wonder why the surfactant concentration variation of the polarizability $\Delta\alpha^e$ (Figure 8) is different: $\Delta\alpha^e$ is sensitive not only to the molecule size but also to the number of condensed counterions (eq 9). This is why $\Delta\alpha^e$ increases with surfactant concentration below the c_{ip}, exhibits a maximum, and decreases afterward, while τ_3 decreases monotonously.

Because the origin of the other relaxation times is unclear, it is difficult to rationalize their variations.

4.4. Birefringence Buildup. In this section we analyze the time-dependent evolution in the presence of the electric field, i.e., the birefringence buildup process. The characteristic times depend in this case on the interactions between permanent and/or induced dipoles and the electric field.

For dilute solutions of monodisperse, ellipsoidal rigid molecules, and for small electric fields, one can describe the rise of the birefringence as[45]

$$\frac{\Delta n(t)}{\Delta n_0} = 1 - \frac{3r}{2(r+1)}e^{-2D_r t} + \frac{r-2}{2(r+1)}e^{-6D_r t} \qquad (13)$$

where $r = \mu^2/k_B T\Delta\alpha_e$, μ being the permanent dipole moment. When there is no permanent dipole moment, $r = 0$, and this equation reduces to

$$\frac{\Delta n(t)}{\Delta n_0} = 1 - e^{-6D_r t} \qquad (14)$$

DOI: 10.1021/acs.macromol.6b01240
Macromolecules 2016, 49, 5618−5629

Again, as in the case of relaxation, it was impossible to fit the buildup curves with a single exponential except for the smallest applied electric fields ($E < 250$ V mm^{-1}). However, the fits with two characteristic times were satisfactory (see Supporting Information):

$$\frac{\Delta n(t)}{\Delta n_0} = 1 - A_1 e^{-t/\tau_1} - A_2 e^{-t/\tau_2} \quad (15)$$

Figure 9 shows the variation of the rise times with electric field. The decay times are also plotted for the sake of comparison. The ratio between the two buildup times is generally higher than 3 as in eq 12, even for small values of E. Furthermore, the buildup times appreciably depend on the amplitude of the electric field, at the difference of relaxation times. This is in fact expected as the linear electric field regime is observed below 200 V/mm (see Figure 2). Close to saturation, O'Konski et al. showed that in the case of monodisperse rods there are two buildup times: one associated with permanent dipoles $\tau_p = 1/(2D_r)(k_BT/\mu E)$ and one to the induced dipoles $\tau_i = (1/2D_r)(k_BT/\Delta\alpha^e E^2)$.[68] Here, we assumed that there were no (or negligible) permanent dipole moments. The fact that the fits of the buildup curves require two times might be associated with two types of induced dipole moments or to two different alignment processes, possibly corresponding to two of the three relaxation times found during the decay process. Because the fields used are outside the linear regime, it is not easy to extrapolate the buildup times to zero field. We can only say from Figure 9 that the buildup times become closer to the relaxation times as the field decreases.

In the presence of DTAB, the fitting of the buildup curves also requires two relaxation times, as in the absence of DTAB. The shorter one (τ_1) decreases when the field increases while the longer one (τ_2) is rather independent of the electric field (within error bars). The times and the amplitude ratio A_1/A_2 can be found in the Supporting Information for both polymer concentrations and various DTAB concentrations, below and above the isoelectric point.

For solutions with 115 mg L^{-1} polymer and without DTAB, the amplitudes A_1 and A_2 are positive. With DTAB and for small fields, A_1/A_2 becomes negative close to the isoelectric point. At high field, A_1/A_2 becomes negative at smaller DTAB concentrations; the amplitude A_2 becomes more negative as the electric field and the DTAB concentration increase (see Figure 10). Amplitudes of opposite signs result in anomalous Kerr signals as found in other systems (see section 1). The fact that the negative contribution is absent in pure polymer solutions shows that the surfactant plays a role in this anomalous orientation mechanisms. The anomalous signals are observed above E = 150 V/mm (see Supporting Information) for solutions at $c_{DTAB} > c_{ip}$, suggesting the existence of a potential barrier in the mechanism involved in the negative contribution to the birefringence.

For solutions with 60 mg L^{-1} polymer and for all DTAB concentrations, the amplitudes A_1 and A_2 are positive; the ratio A_1/A_2 is positive at all surfactant concentrations showing a minimum at the isoelectric point for both small and high field intensities (see Supporting Information).

This behavior could be rationalized as follows: above the CAC, which is close to the isoelectric point, the surfactant binds to the polyelectrolyte, the polyelectrolyte chains become more hydrophobic, favoring the formation of aggregates. Inside these aggregates, and if the electric field is strong enough, DTAB ions

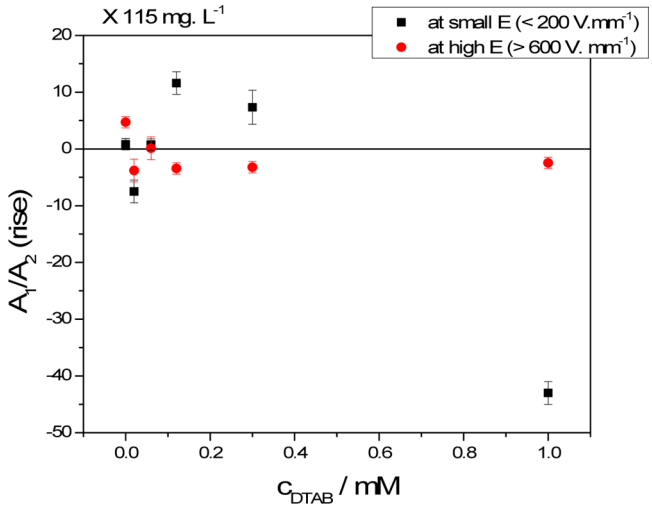

Figure 10. Dependency of the ratio A_1/A_2 on surfactant concentration, c_p = 115 mg L^{-1}.

condensed on a particular chain could overcome the potential that binds them to the molecule and jump to an adjacent molecule producing and effective perpendicular polarization along the cross section of the aggregates. This polarization produces a negative contribution to the birefringence which is field dependent. The fact that a minimum electric field is required (~150 V/mm) is consistent with the idea of an energy barrier for the exchange of surfactant ions. Anomalous signals are not seen for the lowest polymer concentration because the aggregation is negligible in this case. Let us recall that the diameter of the aggregates should be larger than their length, for the Manning threshold of the anomalous behavior to be reached.[27]

The results are consistent with the idea that the anomalies are a consequence of a collective behavior due to interactions among chains,[27] here mediated by surfactant ions.

5. CONCLUSIONS

We have measured the dynamic and stationary Kerr effect on solutions of a rod-like polyelectrolyte and in its mixtures with an oppositely charged surfactant. We found that at low polymer concentration no anomalous birefringence signals are found whatever the surfactant concentration or the field. At higher polymer concentration and when surfactant is present, anomalous signals appear evidencing a new relaxation process with a negative contribution to the birefringence. When the surfactant concentration is below the CAC (here close to the isoelectric point), these anomalies are present only for the higher field strengths (above the linear Kerr regime), but for surfactant concentrations above the CAC, anomalies are present at all the investigated fields. Above the CAC, the surfactant ions are bound to the polymer backbone. These ions are able to leave the polymer chain when aggregates of parallel rods are formed. This perpendicular polarization produces a torque that tends to orient the chains with their main axes perpendicular to the applied electric field. This leads to a negative contribution to the birefringence and opposes the tendency of chains to orient parallel to the field when the counterions are polarized along the macromolecule backbone.

The negative contribution is especially important at high field strengths and at surfactant concentrations above the CAC. All the results shown here are consistent with the Manning's theory

DOI: 10.1021/acs.macromol.6b01240
Macromolecules 2016, 49, 5618−5629

which ascribes the anomalous signals to the perpendicular polarization of condensed counterions when the formation of aggregates of parallel rods with cross sections of size comparable to the polymer chain length. It is not due to the perpendicular polarization of free counterions as in the case of flexible polyelectrolytes. More experiments are needed to clarify the role of condensed counterions, varying parameters such as charge density, polymer concentration, and polymer backbone rigidity. Work on DNA/DTAB mixed solutions, for which anomalous birefringence signals were also found, is in progress.

■ ASSOCIATED CONTENT

Supporting Information

The Supporting Information is available free of charge on the ACS Publications website at DOI: 10.1021/acs.macromol.6b01240.

Xanthan characteristics and additional experimental data, analysis, and figures (PDF)

■ AUTHOR INFORMATION

Corresponding Author

*E-mail: hernan.ritacco@uns.edu.ar (H.A.R.).

Notes

The authors declare no competing financial interest.

■ ACKNOWLEDGMENTS

We are deeply grateful to Professor David Kurlat for years of discussions on the Kerr effect; this paper is dedicated to his memory. We thank Roland Netz for very useful discussions concerning the mechanisms of dielectric relation in polyelectrolyte solutions and their eventual contribution to electric birefringence. We also thank Eduardo Acosta for helping us with the Kerr effect apparatus. Support from Agencia Nacional de Promoción Científica y Tecnológica (ANPCyT, Argentina) under grant PICT 2013 (D) no. 2070; and Consejo Nacional de Investigaciones Científicas y Técnicas (CONICET, Argentina) under grant PIP GI no. 11220130100668CO, is gratefully acknowledged. This work was partially supported by grants PGI-UNS 24/F067 and PGIMayDS 24/MA09 of Universidad Nacional del Sur (Argentina). C.D. is grateful to CIC for her fellowship.

■ REFERENCES

(1) Dobrynin, A. V.; Rubinstein, M. Theory of polyelectrolytes in solutions and at surfaces. *Prog. Polym. Sci.* **2005**, *30* (11), 1049−118.

(2) Kwak, J. C. T., Ed.; *Polymer-Surfactant Systems*; Marcel Dekker: 1998.

(3) Decher, G.; Schlenoff, J. B. *Multilayer Thin Films. Sequential Assembly of Nanocomposite Materials*; Wiley-VCH Verlag GmbH & Co.: 2002.

(4) Imai, N.; Onishi, T. Analytical Solution of Poisson-Boltzmann Equation for Two-Dimensional Many-Center Problem. *J. Chem. Phys.* **1959**, *30* (4), 1115−6.

(5) Oosawa, F. *Polyelectrolytes*; Marcel Dekker: New York, 1971.

(6) Manning, G. S. Limiting Laws and Counterion Condensation in Polyelectrolyte Solutions I. Colligative Properties. *J. Chem. Phys.* **1969**, *51* (3), 924−33.

(7) Manning, G. S. Limiting Laws and Counterion Condensation in Polyelectrolyte Solutions II. Self-Diffusion of the Small Ions. *J. Chem. Phys.* **1969**, *51* (3), 934−8.

(8) Manning, G. S. Polyelectrolytes. *Annu. Rev. Phys. Chem.* **1972**, *23* (1), 117−40.

(9) Tanigawa, M.; Yamaoka, K. Electrooptical and hydrodynamic properties of synthetic polyribonucleotides in solutions as studied by electric birefringence. *Bull. Chem. Soc. Jpn.* **1995**, *68* (2), 481−92.

(10) Tricot, M.; Houssier, C. Electrooptical studies on sodium poly(styrenesulfonate) 0.1. electric polarizability and orientation function from electric birefringence measurements. *Macromolecules* **1982**, *15* (3), 854−65.

(11) Wijmenga, S. S.; Vandertouw, F.; Mandel, M. The electric birefringence relaxation of aqueous poly-electrolyte solution observed with pulsed rectangular waves of various frequencies. *Polym. Commun.* **1985**, *26* (6), 172−5.

(12) Wijmenga, S. S.; Mandel, M. Influence of some factors affecting the stationary value of the electric birefringence of aqueous-solutions of poly(styrene sulfonates) in the presence of 0.01 mol dm-3 nacl. *J. Chem. Soc., Faraday Trans. 1* **1988**, *84*, 2483−98.

(13) Ookubo, N.; Hirai, Y.; Ito, K.; Hayakawa, R. Anisotropic counterion polarizations and their dynamics in aqueous poly-electrolytes as studied by frequency-domain electric birefringence relaxation spectroscopy. *Macromolecules* **1989**, *22* (3), 1359−66.

(14) Ito, K.; Yagi, A.; Ookubo, N.; Hayakawa, R. Crossover-behavior in high-frequency dielectric-relaxation of linear polyions in dilute and semidilute solutions. *Macromolecules* **1990**, *23* (3), 857−62.

(15) Nagamine, Y.; Ito, K.; Hayakawa, R. Low- and high-frequency electric birefringence relaxations in linear polyelectrolyte solutions. *Langmuir* **1999**, *15* (12), 4135−8.

(16) Bordi, F.; Cametti, C.; Colby, R. H. Dielectric spectroscopy and conductivity of polyelectrolyte solutions. *J. Phys.: Condens. Matter* **2004**, *16* (49), R1423−R63.

(17) Mandel, M. The electric polarization of rod-like, charged macromolecules. *Mol. Phys.* **1961**, *4* (6), 489−96.

(18) Oosawa, F. Counterion fluctuation and dielectric dispersion in linear polyelectrolytes. *Biopolymers* **1970**, *9* (6), 677.

(19) Minakata, A.; Imai, N.; Oosawa, F. Dielectric properties of polyelectrolytes 0.2. theory of dielectric increment due to ion fluctuation by a matrix-method. *Biopolymers* **1972**, *11* (2), 347.

(20) Warashina, A.; Minakata, A. Dielectric properties of polyelectrolytes 0.4. calculation of dielectric dispersion by a stochastic-model. *J. Chem. Phys.* **1973**, *58* (11), 4743−9.

(21) Manning, G. S. Limiting laws and counterion condensation in polyelectrolyte solutions 0.5. further development of chemical-model. *Biophys. Chem.* **1978**, *9* (1), 65−70.

(22) Manning, G. S.; Ray, J. Fluctuations of Counterions Condensed on Charged Polymers. *Langmuir* **1994**, *10* (3), 962−6.

(23) Manning, G. S. A counterion condensation theory for the relaxation, rise, and frequency dependence of the parallel polarization of rodlike polyelectrolytes. *Eur. Phys. J. E: Soft Matter Biol. Phys.* **2011**, *34* (12), 132.

(24) Dhont, J. K. G.; Kang, K. Electric-field-induced polarization of the layer of condensed ions on cylindrical colloids. *Eur. Phys. J. E: Soft Matter Biol. Phys.* **2011**, *34* (4), 40.

(25) Ritacco, H. A.; Kurlat, D.; Rubio, R. G.; Ortega, F.; Langevin, D. Stationary Electric Birefringence of Flexible Polyelectrolyte Solutions: Experimental Evidence of Different Counterion Polarization Mechanisms. *Macromolecules* **2009**, *42* (15), 5843−50.

(26) Kramer, H.; Graf, C.; Hagenbuchle, M.; Johner, C.; Martin, C.; Schwind, P.; et al. Electrooptic effects of aqueous fd-virus suspensions at very-low ionic-strength. *J. Phys. II* **1994**, *4* (6), 1061−74.

(27) Manning, G. S. Transverse polarizability of an aligned assembly of charged rods. *Eur. Phys. J. E: Soft Matter Biol. Phys.* **2009**, *30* (4), 411−5.

(28) Mantegazza, F.; Caggioni, M.; Jimenez, M. L.; Bellini, T. Anomalous field-induced particle orientation in dilute mixtures of charged rod-like and spherical colloids. *Nat. Phys.* **2005**, *1* (2), 103−6.

(29) Hoffmann, H.; Graebner, D. Electric birefringence anomaly of solutions of ionically charged anisometric particles. *Adv. Colloid Interface Sci.* **2015**, *216*, 20−35.

(30) Ritacco, H.; Kurlat, D. H. Critical aggregation concentration in the PAMPS(10%)/DTAB system. *Colloids Surf., A* **2003**, *218* (1−3), 27−45.

DOI: 10.1021/acs.macromol.6b01240
Macromolecules 2016, 49, 5618−5629

(31) Stubenrauch, C.; Albouy, P. A.; von Klitzing, R.; Langevin, D. Polymer/surfactant complexes at the water/air interface: A surface tension and X-ray reflectivity study. *Langmuir* **2000**, *16* (7), 3206−3213.
(32) Holzwarth, G.; Prestridge, E. B. Multistranded helix in xanthan polysaccharide. *Science* **1977**, *197* (4305), 757−9.
(33) Morris, E. R.; Rees, D. A.; Young, G.; Walkinshaw, M. D.; Darke, A. Order-disorder transition for a bacterial polysaccharide in solution - role for polysaccharide conformation in recognition between xanthomonas pathogen and its plant host. *J. Mol. Biol.* **1977**, *110* (1), 1−16.
(34) Paradossi, G.; Brant, D. A. Light-scattering study of a series of xanthan fractions in aqueous-solution. *Macromolecules* **1982**, *15* (3), 874−9.
(35) Morris, V. J.; Franklin, D.; Ianson, K. Rheology and microstructure of dispersions and solutions of the microbial polysaccharide from xanthomonas-campestris (xanthan gum). *Carbohydr. Res.* **1983**, *121* (SEP), 13−30.
(36) Norton, I. T.; Goodall, D. M.; Frangou, S. A.; Morris, E. R.; Rees, D. A. Mechanism and dynamics of conformational ordering in xanthan polysaccharide. *J. Mol. Biol.* **1984**, *175* (3), 371−94.
(37) Sato, T.; Norisuye, T.; Fujita, H. Double-stranded helix of xanthan - dimensional and hydrodynamic properties in 0.1-m aqueous sodium-chloride. *Macromolecules* **1984**, *17* (12), 2696−700.
(38) Kitamura, S.; Takeo, K.; Kuge, T.; Stokke, B. T. Thermally induced conformational transition of double-stranded xanthan in aqueous salt-solutions. *Biopolymers* **1991**, *31* (11), 1243−55.
(39) Gamini, A.; Mandel, M. Physicochemical properties of aqueous xanthan solutions - static light-scattering. *Biopolymers* **1994**, *34* (6), 783−97.
(40) Milas, M.; Rinaudo, M.; Duplessix, R.; Borsali, R.; Lindner, P. Small-angle neutron-scattering from polyelectrolyte solutions - from disordered to ordered xanthan chain conformation. *Macromolecules* **1995**, *28* (9), 3119−24.
(41) Rodd, A. B.; Dunstan, D. E.; Boger, D. V. Characterisation of xanthan gum solutions using dynamic light scattering and rheology. *Carbohydr. Polym.* **2000**, *42* (2), 159−74.
(42) Capron, I.; Brigand, G.; Muller, G. About the native and renatured conformation of xanthan exopolysaccharide. *Polymer* **1997**, *38* (21), 5289−95.
(43) Besio, G. J.; Leavesley, I. M.; Prudhomme, R. K.; Farinato, R. Electric birefringence measurements of native, denatured, and renatured xanthan. *J. Appl. Polym. Sci.* **1987**, *33* (3), 825−834.
(44) Chazeau, L.; Milas, M.; Rinaudo, M. Conformations of Xanthan in Solution: Analysis by Steric Exclusion Chromatography. *Int. J. Polym. Anal. Charact.* **1995**, *2* (1), 21−9.
(45) Déjardin, J. L. *Dynamic Kerr Effect: The use and limits of the Smoluchowski equation and nonlinear inertial responses*; World Scientific: 1995.
(46) Degiorgio, V.; Bellini, T.; Piazza, R.; Mantegazza, F.; Goldstein, R. E. Stretched-exponential relaxation of electric birefringence in polymer-solutions. *Phys. Rev. Lett.* **1990**, *64* (9), 1043−6.
(47) Camesano, T. A.; Wilkinson, K. J. Single molecule study of xanthan conformation using atomic force microscopy. *Biomacromolecules* **2001**, *2* (4), 1184−91.
(48) Odijk, T. Polyelectrolytes near the rod limit. *J. Polym. Sci., Polym. Phys. Ed.* **1977**, *15* (3), 477−83.
(49) Skolnick, J.; Fixman, M. Electrostatic persistence length of a wormlike polyelectrolyte. *Macromolecules* **1977**, *10* (5), 944−8.
(50) Barrat, J. L.; Joanny, J. F. Theory of polyelectrolyte solutions. *Adv. Chem. Phys.* **1996**, *94*, 1−66.
(51) von Klitzing, R.; Espert, A.; Colin, A.; Langevin, D. Comparison of different polymer-like structures in the confined geometry of foam films. *Colloids Surf., A* **2001**, *176* (1), 109−116.
(52) Jain, N.; Trabelsi, S.; Guillot, S.; McLoughlin, D.; Langevin, D.; Letellier, P.; et al. Critical aggregation concentration in mixed solutions of anionic polyelectrolytes and cationic surfactants. *Langmuir* **2004**, *20* (20), 8496−503.
(53) Ritacco, H.; Albouy, P. A.; Bhattacharyya, A.; Langevin, D. Influence of the polymer backbone rigidity on polyelectrolyte-surfactant complexes at the air/water interface. *Phys. Chem. Chem. Phys.* **2000**, *2* (22), 5243−51.
(54) Li, Y. M.; Xu, G. Y.; Chen, A. M.; Yuan, S. L.; Cao, X. R. Aggregation between xanthan and nonyphenyloxypropyl beta-hydroxyltrimethylammonium bromide in aqueous solution: MesoDyn simulation and binding isotherm measurement. *J. Phys. Chem. B* **2005**, *109* (47), 22290−5.
(55) Yamaoka, K.; Ueda, K. Reversing pulse electric birefringence of sodium poly(styrenesulfonate) in aqueous-solutions. *J. Phys. Chem.* **1980**, *84* (11), 1422.
(56) Krause, S. *Molecular Electro-Optics: Electro-Optic Properties of Macromolecules and Colloids in Solution*; Plenum Press: New York, 1981.
(57) Stoylov, S. P.; Stoimenova, M. V. *Molecular and Colloidal Electro-Optics*: CRC Press: Boca Raton, FL, 2007.
(58) Lewis, R. J.; Pecora, R.; Eden, D. Transient electric birefringence measurements of the rotational and internal motions of a 1010 base pair DNA fragment - field-strength and pulse length effects. *Macromolecules* **1987**, *20* (10), 2579−87.
(59) Forster, S.; Schmidt, M. Polyelectrolytes in solution. *Adv. Polym. Sci.* **1995**, *120*, 51−133.
(60) Broersma, S. Rotational diffusion constant of a cylindrical particle. *J. Chem. Phys.* **1960**, *32* (6), 1626−31.
(61) Doi, M.; Edwards, S. F. *The Theory of Polymer Dynamics*; Oxford University Press: New York, 1986.
(62) Degiorgio, V.; Mantegazza, F.; Piazza, R. Transient electric birefringence measurement of the persistence length of sodium polystyrene sulfonate. *Europhys. Lett.* **1991**, *15* (1), 75−80.
(63) Degiorgio, V.; Bellini, T.; Mantegazza, F. Measurements of the Persistence Length of Flexible Polyelectrolytes. *Int. J. Polym. Anal. Charact.* **1995**, *2* (1), 83−93.
(64) Tomic, S.; Babic, S. D.; Vuletic, T.; Krca, S.; Ivankovic, D.; Griparic, L.; et al. Dielectric relaxation of DNA aqueous solutions. *Phys. Rev. E* **2007**, *75* (2), 021905.
(65) Kim, W. K.; Netz, R. R. Barrier-induced dielectric counterion relaxation at super-low frequencies in salt-free polyelectrolyte solutions. *Eur. Phys. J. E: Soft Matter Biol. Phys.* **2015**, *38* (11), 120.
(66) van den Heuvel, M. G. L.; Bondesan, R.; Lagomarsino, M. C.; Dekker, C. Single-molecule observation of anomalous electrohydrodynamic orientation of microtubules. *Phys. Rev. Lett.* **2008**, *101* (11), 118301.
(67) Schlagberger, X.; Netz, R. R. Anomalous birefringence and polarizability saturation of charged elastic rods: Field-strength, salt and finite-concentration effects. *Europhys. Lett.* **2008**, *83* (3), 36003.
(68) O'Konski, C. T.; Yoshioka, K.; Orttung, W. H. Electric properties of macromolecules 0.4. determination of electric and optical parameters from saturation of electric birefringence in solutions. *J. Phys. Chem.* **1959**, *63* (10), 1558−65.
(69) Manning, G. S. Ionic polarizability of interacting charged rods. *Europhys. Lett.* **2009**, *86* (3), 36001.

NOTE ADDED AFTER ASAP PUBLICATION

This paper was published ASAP on July 29, 2016 with text errors in the Discussion section. The corrected version was reposted on August 9, 2016.

DOI: 10.1021/acs.macromol.6b01240
Macromolecules 2016, 49, 5618−5629